



Synthesis, Electric and Magnetic Characterization of Nickel Ferrite/PANI Nano-Composite Prepared by Flash Auto Combustion Method

A. M. A. Henaish^{1,2} · M. M. Ali¹ · D. E. El Refaay^{3,4} · I. A. Weinstein^{2,5} · O. M. Hemedat¹

Received: 30 June 2020 / Accepted: 29 August 2020 / Published online: 8 September 2020
© Springer Science+Business Media, LLC, part of Springer Nature 2020

Abstract

NiFe₂O₄/PANI nano-composite with different polyaniline (PANI) content (25%, 50% and 75%) is synthesized. The NiFe₂O₄ (NF) is prepared by the flash auto combustion method and annealed at 400 °C for 2 h. The PANI is prepared by oxidative polymerization of aniline. The X-ray diffraction (XRD) technique confirmed that the NiFe₂O₄ particles are successfully dispersed in the PANI matrix with single phase structure. The characteristic absorption bands are observed from infrared (IR) spectra for the pure NF, pure PANI and their nano-composite. The dielectric constant (ϵ') behavior of NF/PANI nano-composite at higher PANI content tends to be a polymer behavior. The Curie temperature decreased by increasing the PANI content and it is attributed to the basis of A-B exchange interaction due to the variation of Fe³⁺ content among the octahedral and tetrahedral sites. The values of the saturation magnetization (Ms), remanence magnetization (Mr), coercivity (Hc), area and squareness (Mr/Ms) are measured by using a vibrating sample magnetometer (VSM).

Keywords Ni ferrite · PANI · Flash auto combustion · XRD · DC resistivity · Dielectric constant · VSM

1 Introduction

In the last decades, Microwave absorption materials have attracted greater interest due to its ability to absorb electromagnetic (EM) wave effectively and convert it into thermal energy by interference [1–3]. Microwaves absorbing materials can be classified into dielectric loss materials as conducting polymers (CPs) and magnetic loss materials according to different absorbing mechanisms as in ferrite [4–6].

Conducting polymers (CPs) such as PANI have become an expanding research area and PANI is the most promising conductive polymer with excellent environmental stability,

electrochemical activity, high electrical conductivity, facile synthesis, and low synthetic cost, which could be used as microwave absorbing materials [7, 8].

NiFe₂O₄ is one of the most important spinel ferrites which, has known as a soft ferrite with low coercivity, saturation magnetization, chemical stability and high electrical resistivity so it can be used as a magnetic resonance imaging (MRI) enhancement, magnetic recording media, color imaging, ferro-fluids, high frequency devices, magnetic refrigerators, catalysts, microwave devices and electronic devices [9–11].

Nowadays Polymer nanocomposites (combination of polymers and organic/inorganic fillers at the nanometer scale) have attracted many scientific researches due to its novel features. These novel materials can be used as applications in many industrial fields. PANI is considered as an example for the polymer nanocomposite and can be synthesized by polymerization of aniline in the presence of dispersed inorganic material [12, 13]. C. Wang et al. [13] prepared NiZn-ferrite/PANI by using hydrothermal method, the prepared samples showed a high saturation magnetization and coercivity at room temperature. Also, M.Ajmal et al. [8] studied the optical and dielectric properties of NiZn ferrite/PANI, they found that the optical band gap and the dielectric decreases as the amount of ferrite increases. Many authors

✉ A. M. A. Henaish
ahmed.henaish@science.tanta.edu.eg

¹ Physics Department, Faculty of Science, Tanta University, Tanta 31527, Egypt

² NANOTECH Center, Ural Federal University, Ekaterinburg 620002, Russia

³ Physics Department, Faculty of Science, King Khalid University, Abha, Saudi Arabia

⁴ Physics Department, Faculty of Science, Suez University, Suez, Egypt

⁵ Institute of Metallurgy of the Ural Branch of the Russian Academy of Sciences, Ekaterinburg 620016, Russia

[14–17] studied the effect of nickel ferrite/PANI with different content of other doping materials. M. Khairy et al. [4] prepared Ni-ferrite by sol gel method and added the PANI with 2.5%, 5% and 50%. They found that the electrical conductivity increases as the Ni-ferrite percent increases and the optical absorption band observed in near infrared with energy gap 1 eV. According to the above review, we decided to focus on the synthesis of nickel ferrite/PANI nano-composite through the flash auto combustion method with different percentage and study the effect of PANI addition on the structural, magnetic, and electrical properties.

2 Experimental Details

NiFe₂O₄ nano-powder is prepared by the flash auto combustion method. Nickel nitrate Ni(NO₃)₃·6H₂O, ferric nitrate Fe(NO₃)₃·9H₂O and urea CO(NH₂)₂ as a fuel are used for preparation [18]. The metal nitrates are mixed with the urea by using a glass rod. The mixture is heated at 80 °C with constant stirring on a hot plate until the mixture become viscous. The internal ignition takes the form of a tree, and finally forms a brown ferrite powder. The powder is collected and annealed at 400 °C for 2 h. The PANI synthesis is carried out by the polymerization of aniline monomer (ANIHCl) with ammonium persulfate (APS) using a magnetic stirring. Both components are dissolved in (0.1 M) hydrochloric acid and slowly added to each other by stirring for 10 h, while keeping the temperature at 0 °C. The resulting polymer precipitate is collected by filtration and washed with distilled water several time and finally dried at 80 °C overnight [19].

Ni ferrite is incorporated in PANI with different PANI content (25%, 50% and 75%). The Ni ferrite and PANI are mixed for one hour in distilled water and stirred by using a magnetic stirrer. Then the mixture is dried at 80 °C for 24 h as shown in Fig. 1. For electrical measurement, all samples are pressed as pellets under 15 Ton/cm². The XRD is used for characterization the structure of all the prepared samples and carried out using Shimadzu XRD6000, Japan. The XRD data are taken at room temperature using Cu-K α radiation source ($\lambda = 1.5405 \text{ \AA}$) in the range of 2θ (2–80°) with 0.02° increment. The IR spectra carried out on all investigated samples using the infrared spectrometer Perkin-Elmer 1430, Germany in the wavenumber range from 200–4000 cm⁻¹ in the KBr medium.

The behavior of dielectric constant is studied in the temperature range (300 – 800 K) at different frequencies (100 Hz and 1 kHz) using RLC-Bridge (MC2811C LCR meter). The magnetizations of the prepared samples are investigated using vibrating sample magnetometer (VSM, operating system v 1.6 control software Oxford OX8JTL England).

3 Results and Discussion

3.1 X-Ray Diffraction Analysis (XRD)

The X-ray is done at room temperature for pure NiFe₂O₄ (NF), pure polyaniline (PANI) and their intermediate composites (Ni-PANI composite) with different ratio (25%, 50% and 75% PANI are done by weight) and the patterns are shown in Fig. 2. The XRD patterns confirm that NF-PANI composite are more packed than pure PANI. The broadening nature of different peaks reflects the small dimensions of the prepared particles which is measured by Scherer's equation [20] and is found to be around 17–22 nm. The Scherer's equation is given by

$$t = \frac{0.9\lambda}{h_{1/2} \cos \theta} \quad (1)$$

where λ is the wavelength of Cu-K α ($\lambda = 1.540598 \text{ \AA}$), $h_{1/2}$ is the full width at half maximum (FWHM) in radian, and θ is the diffraction angle. The XRD pattern for PANI is shown in Fig. 2 and shows amorphous nature of PANI in partially crystalline state with two different peaks at about $2\theta = 20.3$ (100) plane and $2\theta = 25.1$ (110) plane [21].

However, XRD patterns of NF-PANI composite show different peaks almost similar to the pure PANI. The diffraction peak at 25.1 appears at all composite ratio whereas the first diffraction peak which belongs to the benzenoid ($2\theta = 20.3$) disappears. This may be due to the transformation of PANI skeleton rings by the addition of ferrite. At high concentrations of PANI (25%, 50% and 75%), the two crystalline states of ferrite and PANI still present with small shift of the main diffraction peak (311) leading a variation in the lattice parameter. The calculated lattice parameter and the particle size of NF-PANI composite are given in Table 1. It is noticed that the XRD patterns have no additional peaks for any foreign phases indicating a single phase of NF. The intensity of the peaks characterized for the PANI structure is weakened by increasing the ratio of NF in our nano composite and one of them (100) is completely disappeared at higher ratio. This disappearance is due to the absorption of PANI on the NF surface by the strong adhesion force [22].

3.2 FTIR Spectroscopic Analysis

The IR spectroscopy is a useful technique for confirming the cation distribution in the crystal lattice through their vibrational modes [23]. The FTIR spectra for the pure NF, pure PANI and their nano composite with ratios 25%, 50% and 75% are shown in Fig. 3. The characteristic absorption bands of PANI occur at 1577, 1494, 1301, 1240, 1139 and

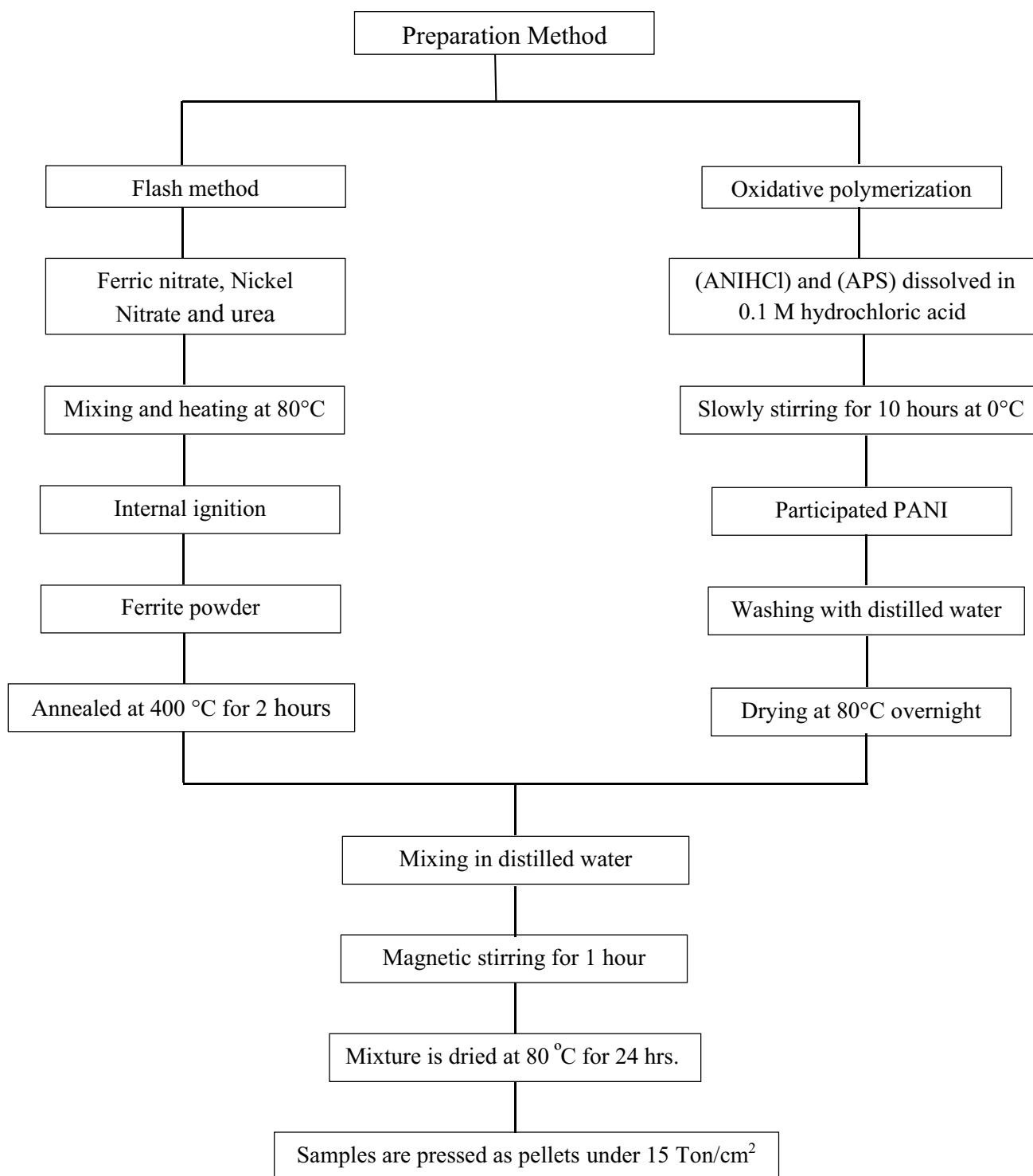


Fig. 1 Sample preparation flow chart

805 cm^{-1} . The absorption bands at 1577 and 1494 cm^{-1} are assigned to the stretching vibration of $\text{C}=\text{C}$ bond of the quinonoid and benzenoid ring while the peak at 1301 and 1240 cm^{-1} are assigned to the stretching vibration of $\text{C}-\text{N}$. The broad absorption band at 1139 describes the

electronic light band and is attributed to the vibration mode of $\text{N}=\text{Q}=\text{N}$, where Q refers to the quinonoid ring. Finally, the peak at 805 cm^{-1} is assigned to the out plane deformation of $\text{C}-\text{H}$ in the benzene ring.

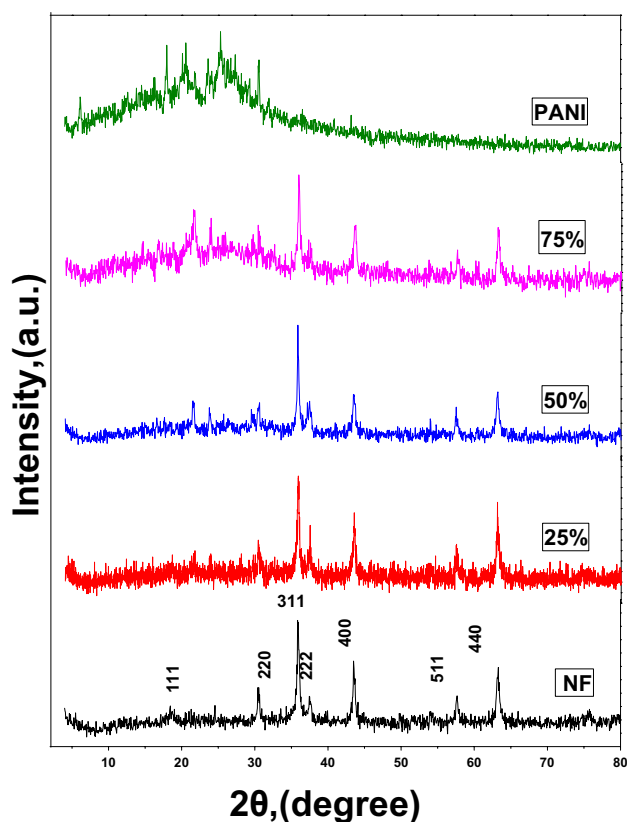


Fig. 2 XRD for (NF), (PANI) and their composites (NF/PANI)

Table 1 Values of lattice parameter, particle size for (NF) and their composites (NF/PANI)

Composition	Lattice parameter a (Å)	Particle size d (nm)
75%	8.1198	16.6084
50%	8.1905	22.014
25%	8.1240	19.0856
NF	8.2973	17.0808

The broad absorption bands for NF appear at the far infra-red due to the stretching vibration of $\text{Fe}^{+3}\text{O}^{-2}$ at the octahedral and the tetrahedral sites, which are assigned by (ν_1) for the tetrahedral site and (ν_2) for the octahedral site. The highest band (ν_1) is observed at around 600 cm^{-1} , while the lowest band is usually observed at 420 cm^{-1} and is assigned for the octahedral site. The absorption band located at 3400 cm^{-1} is due to the stretching vibration of H–O. The FTIR spectra for the NF/PANI nano composite are almost identical to both constituents of our composite, but the ferrite absorption bands are getting weaker by increasing the PANI ratios which indicates a variation in the ferrite molecular structure because of the adding PANI.

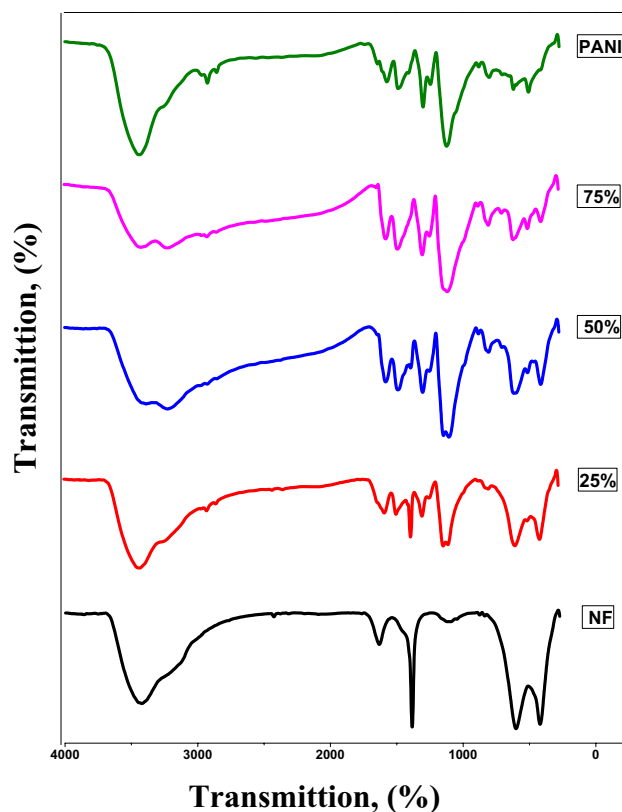


Fig. 3 FTIR for (NF), (PANI) and their composites (NF/PANI)

Table 2 IR absorption data for (NF), (PANI) and their composites (NF/PANI)

Composition	$\nu_1(\text{cm}^{-1})$	$\nu_2(\text{cm}^{-1})$	$\mathcal{F}_{\text{tet}}(\text{dyne/cm})$	$\mathcal{F}_{\text{oct}}(\text{dyne/cm})$
PANI	503.408	615.2764	1.86×10^5	2.77×10^5
75%	405.0409	505.3367	1.20×10^5	1.87×10^5
50%	408.898	507.256	1.22×10^5	1.88×10^5
25%	412.756	597.9175	1.25×10^5	2.62×10^5
NF	420.471	601.775	1.29×10^5	2.65×10^5

The Force constant in unit dyne/cm for ($\text{Fe}^{+3} - \text{O}^{-2}$) bonds at both tetrahedral and octahedral site was calculated using the formula [24]

$$\mathcal{F} = 4\pi^2 c^2 \nu^2 \mu \quad (2)$$

where c is the velocity of light in (cm/sec), ν is the wavenumber in cm^{-1} and μ is the reduced mass in gm. It is noticed from Table 2 that the force constant of the tetrahedral site increases by increasing Ni content. This increase of the force constant can be attributed to the increase of the vibrating frequency of the tetrahedral site which shifts to a higher frequency by increasing Ni content. The force constant of the octahedral site decrease by increasing Ni content

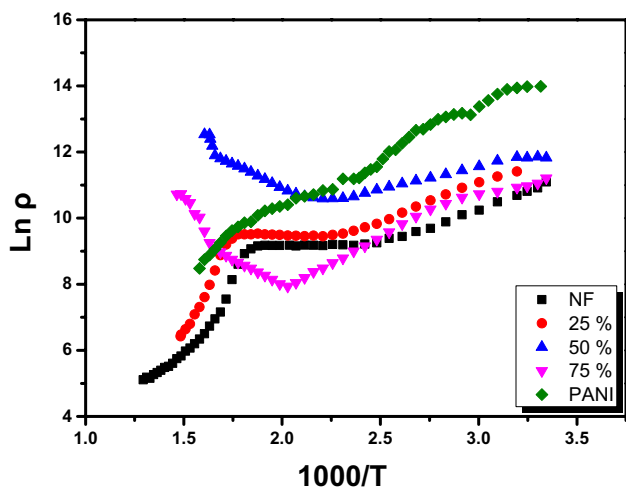


Fig. 4 Variation of ($\ln \rho$) as a function of temperature reciprocal at 100 Hz

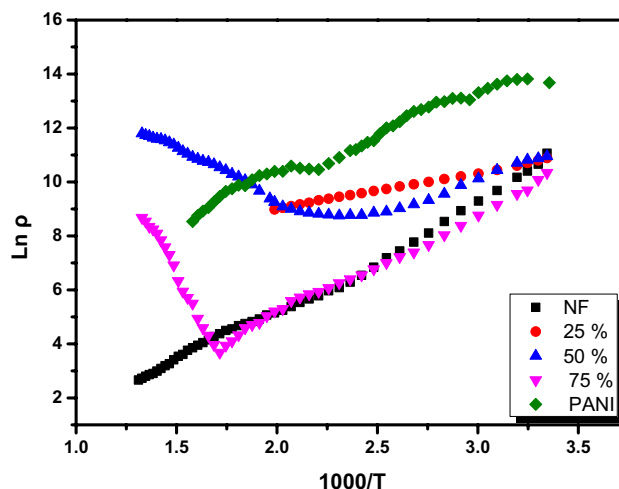


Fig. 6 Dielectric constant as a function of temperature at 100 Hz

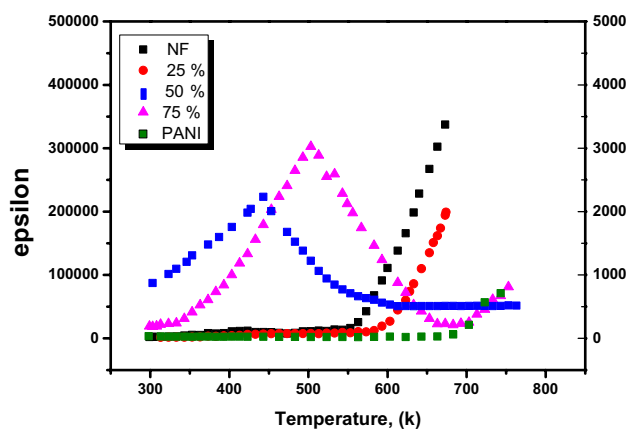


Fig. 5 Variation of ($\ln \rho$) as a function of temperature reciprocal at 1 kHz

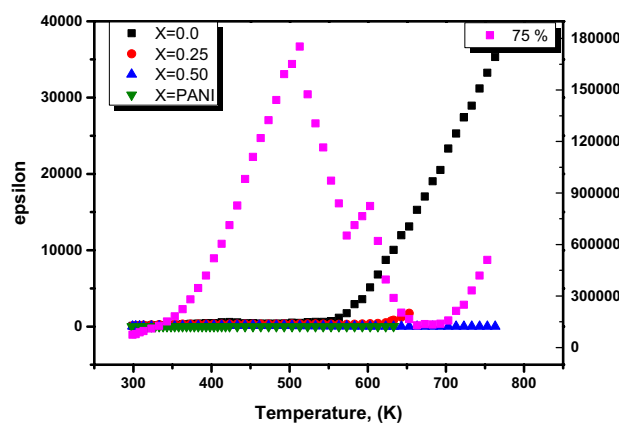


Fig. 7 Dielectric constant as a function of temperature at 1 kHz

up to $x=0.75$ and then slightly increase which have the same behavior of the absorption frequency (ν_2).

3.3 Dielectric Behavior

The variation of the AC resistivity for the prepared samples with temperature in the range (300–800 K) at 100 Hz and 1 kHz is shown in Fig. 4 and Fig. 5 respectively. The relation between resistivity and temperature is given by [25]:

$$\rho = \rho_0 e^{\frac{\Delta E}{kT}} \tag{3}$$

where (ρ) is the resistivity at temperature (T), (ΔE) is the activation energy for electrical process. The AC resistivity for the prepared nano composite samples is measured using RLC bridge (from room temperature to 800 K) and

two different frequencies (100 Hz and 1 kHz). It is shown that the AC resistivity decrease by increasing temperature in the low temperature region when the predominant mechanism belongs to ferrite hopping conduction. Above certain temperature the composite obeys the conduction mechanism, and change the slope or behavior of $\ln \rho$ versus $1000/T$ due to the contribution of polyaniline which has a semiconductor character. It can be said that this temperature is the transition temperature between two conduction mechanism (hopping and semiconductor mechanism). At samples ($X=0.5$ and 0.75) the $\ln \rho$ has minimum values near the PANI glass transition temperature. For pure ferrite the change in the slope is due to transition from ferromagnetic to paramagnetic state.

The dielectric constant (ϵ') behavior of NF/PANI nano composite as a function of temperature (from room temperature to 800 K) at 100 Hz and 1 kHz is shown in Fig. 6 and Fig. 7 respectively. At low PANI concentration, the dielectric constant increases gradually up to a certain temperature

(about 600 K) and then increases rapidly which is a characteristic phenomenon of ferrite.

The dielectric constant of ferrite is attributed to four types of polarization mechanisms (interfacial, dipolar, atomic and electronic polarization). At low frequencies, all types of polarization contribute to the dielectric value. At higher frequencies, only the atomic and the electronic polarizations are responsible for the dielectric values. At higher temperatures, the rapid increase of ϵ' with temperature is due to the interfacial and dipolar polarization which are strongly dependent on temperature [26, 27]. The interfacial polarization results from the accumulation of charges at the grain boundary which increases by increasing the temperature and appears at low frequency [28, 29].

At higher PANI content ($X=0.5$ and 0.75), the behavior of dielectric constant with temperature tends to be a polymer behavior which is a peak at a certain temperature (around the glass transition temperature for polymer) as shown in the figures. Below that temperature, the dielectric constant increases due to the wagging vibration of polymer chain which increases the polarization. Above that temperature, the dielectric constant decreases due to the suppression process occurred by the polymer which decreases the hopping process and consequently decreases the polarization and dielectric constant value. The behavior of the dielectric constant may be explained quantitatively by the suggestion that the mechanism of polarization process in ferrite is similar to the conduction process. The dielectric conduction mechanism can be explained according to the electron hopping model as follows [30].



In this model, the electron hopping occurred between two adjacent iron ions in the spinel lattice especially at the octahedral site causes a local electron displacement in the direction of the applied electric field and enhance the polarization of ferrite. From the Fig. 6 and Fig. 7, it is noticed that the dielectric constant decreases by increasing the external applied frequency.

3.4 DC Resistivity

The DC resistivity is plotted as a function of the temperature reciprocal ($1000/T$) as shown in Fig. 8.

It is shown that at low concentration of PANI ($X=0$, $X=0.25$ and $X=0.50$), the temperature dependence of DC resistivity has a linear relation with two regions and one break point. The transition from ferromagnetic to paramagnetic state occurs at Curie temperature which is shifted to higher temperature with the increase of PANI content. The decrease of Curie temperature by increasing the PANI content may be explained on the basis of

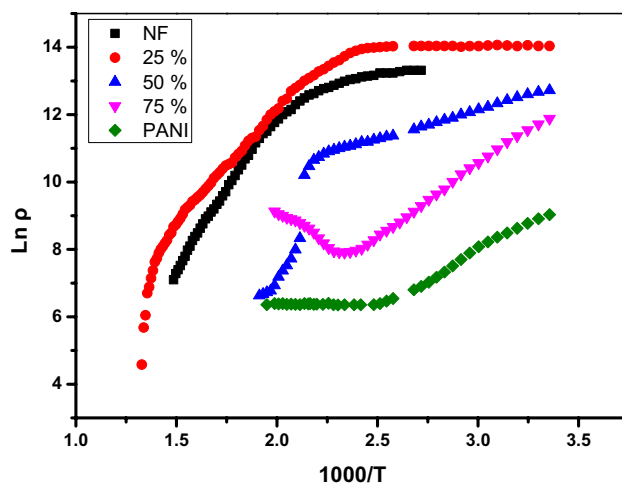


Fig. 8 Variation of DC resistivity as a function of temperature reciprocal

Table 3 Activation energy for ferrimagnetic and paramagnetic regions

Composition	E_g (eV)	E_p (eV)
NF	0.13	0.79
25%	0.55	2.03
50%	0.13	0.89

A-B exchange interaction due to the variation of Fe^{3+} content among the octahedral and tetrahedral sites [31]. The first region of DC resistivity belongs to the ferromagnetic phase in which obeys the hopping conduction mechanism. The second disorder region belongs to the paramagnetic phase. The activation energy for the ferrimagnetic and paramagnetic region is calculated as shown in Table 3. The small values of activation energy indicate the presence of hopping conduction mechanism. The hopping conduction mechanism increases and the activation energy decreases. The electrical resistivity for all samples decreases by increasing the temperature indicating the semiconductor nature for all samples. The conduction mechanism in the first region involves the exchange of electrons between similar ions with difference valence. These hopping electrons are thermally activated and their mobility increases by increasing the temperature leads to the decrease of DC resistivity. At higher PANI content ($X=0.75$), the DC resistivity has a minimum value at certain temperature (around the polymer glass transition temperature). At low temperature, the ferrite mechanism of conduction is the predominant mechanism and the resistivity decreases linearly by increasing the temperature due to the thermally activated hopping electrons. Above the glass transition temperature, the semiconductor nature of polymer is the predominant factor that affects the resistivity at

this region. The resistivity increases due to the suppression of hopping electrons caused by polymer chain at higher temperature. The ease of motion for the polymer chain at higher temperature facilitates the suppression process of the hopping electrons which leads to the increase of resistivity [32].

3.5 VSM Measurements

The room temperature hysteresis loop for Ni-ferrite doped with different content of PANI (25%, 50% and 75%) were shown in Fig. 9. The values of saturation magnetization (M_s), remanence magnetization (M_r), coercivity (H_c), area and squareness (M_r/M_s) of the loops are listed in Table 4. The samples have polycrystalline structure with crystal size less than 40 nm which indicates that the samples have mono domain structure illustrating the easy arrangement of the domain in the direction of the external magnetic field. The low value of coercivity and unsaturated magnetization indicates the presence of mono domain structure, beside the value of M_r/M_s is very small that we can say that the samples are like superparamagnetic material.

The easy arrangement explains the low value of coercivity as shown in Table 4. The values of squareness are very small and ranged from 0.17 to 0.19 which indicate that the samples are still soft magnetic ferrite. The saturation magnetization decreases from 16.9 to 3.63 emu/g. The presence of PANI dilutes the magnetic properties of the composite samples leading to the decrease of saturation magnetization and remanence magnetization. The presence of PANI resists the easy domain motion in the direction of the external magnetic field and rotates the domain at higher values of the external magnetic field. This motion leads to the increase of coercivity from 261 to 290 gauss. The decrease of (M_s) and (M_r) may be also attributed to the decrease of the A-B exchange interaction due to the presence of PANI.

The values of coercivity can be given from the following relation [33]

$$H_c = \frac{2K}{\mu_0 M_s} \quad (5)$$

where K is the magnetic crystalline anisotropy and μ_0 is the permeability of free space. According to the previous equation, the M_s value decreases by increasing the PANI content while H_c and K values increase by increasing the PANI content.

The values of the experimental magnetic moment (μ_{exp}) are calculated by using Eq. (5) [34], while the theoretical magnetic moment (μ_{theo}) values are calculated on the basis of Neel's theory and are done by using Eq. (6).

$$\mu_{exp} = \frac{wM_s}{5585} \quad (6)$$

$$\mu_{theo} = |M_B| - |M_A| \quad (7)$$

where w is the molecular weight of the sample, $|M_B|$ is the magnetic moment at B-site and $|M_A|$ is the magnetic moment at A-site. The theoretical and experimental magnetic moment values are shown in Table 4 and they are close to each other indicating the absence of canting angle for the ionic magnetic moment at B-site, which indicates that the proposed cation distribution $[Fe_1] [Ni_1 Fe_1]$ is correct. The proposed cation distribution is calculated by using the following formula [35] and shown in Table 5:

$$a_{th} = \frac{8}{3\sqrt{3}} \left[(r_A + r_o) + \sqrt{3}(r_B + r_o) \right] \quad (8)$$

where a_{th} is the theoretical lattice parameter, r_o is the oxygen radius, r_A is the tetrahedral site radius and r_B is the octahedral site radius.

4 Conclusion

NiFe₂O₄/PANI nano composite with different polyaniline (PANI) content (25%, 50% and 75%) are successfully synthesized by using flash auto combustion method. The XRD for the studied samples shows both the diffraction peaks of ferrite and the broad peak of polyaniline. The FTIR confirms that the ferrite particle embedded into the polymer chain of polyaniline. The experimental measurements at low PANI concentration show that, the dielectric constant increases gradually up to a certain temperature (about 600 K) then increases rapidly which is a characteristic phenomenon of ferrite. The DC resistivity has a minimum value at a certain temperature (around the polymer glass transition temperature) at higher PANI content. The magnetic parameters of Ni ferrite show that the samples are soft magnetic material, with mono domain structure illustrating the easy arrangement of the domain in the direction of the external magnetic field.

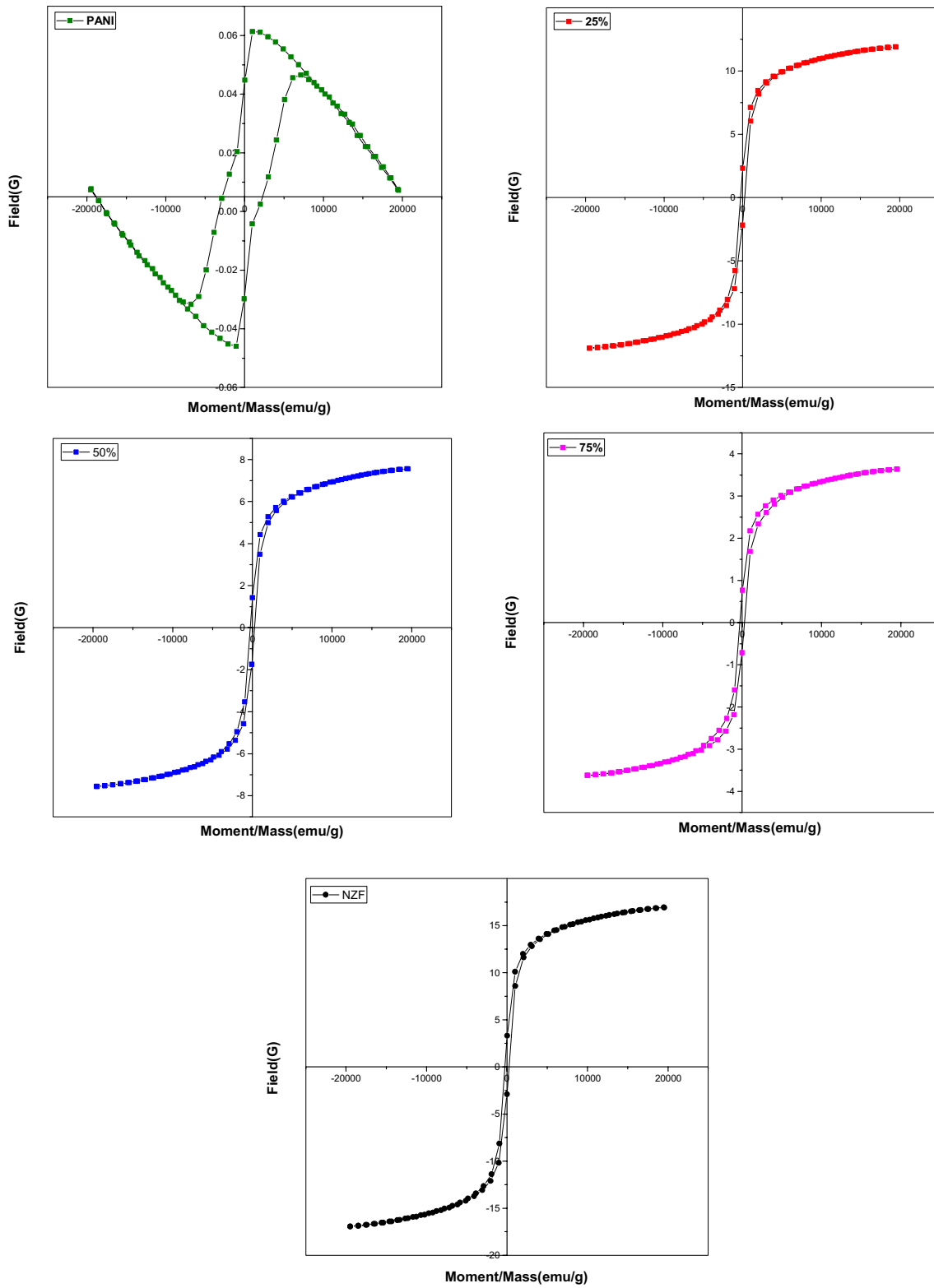


Fig. 9 M-H curves for (NF) and their composites (NF/PANI)

Table 4 Values of saturation, remanence magnetization, coercive field, squareness, experimental, theoretical magnetic moment for (NF) and their composites (NF/PANI)

Composition	M_s (emu/g)	M_r (emu/g)	H_c (G)	M_r/M_s	$(\mu_{exp}) \mu_B$	$(\mu_{th}) \mu_B$	Area ($\times 10^3$)
75%	3.63	0.7	290	0.19	–	–	3
50%	7.55	1.35	265	0.179	–	–	5
25%	11.91	2.13	259	0.177	–	–	8
NF	16.9	3.63	261	0.175	2.1	2	18

Table 5 Calculated cation distribution

Composition	r_A (\AA)	r_B (\AA)	a_{theo} (\AA)	a_{exp} (\AA)
NF	0.69	0.695	8	8.297

References

1. L. Sun, R. Zhang, Z. Wang, L. Ju, E. Cao, Y. Zhang, Structural, dielectric and magnetic properties of NiFe₂O₄ prepared via sol-gel auto-combustion method. *J. Magn. Magn. Mater.* **421**, 65–70 (2017)
2. L. Panbo, H. Ying, Z. Xiang, Cubic NiFe₂O₄ particles on graphene-polyaniline and their enhanced microwave absorption properties. *Compos. Sci. Technol.* **107**, 54–60 (2015)
3. M. Kurian, D.S. Nair, Effect of preparation conditions on Nickel Zinc Ferrite nanoparticles: A comparison between sol-gel auto combustion and co-precipitation methods. *J. of Saudi Chemical Society.* **20**, S517–S522 (2016)
4. M. Khairy, M.E. Gouda, Electrical and optical properties of nickel ferrite/polyaniline nanocomposite. *J. of Adv. Res.* **6**, 555–562 (2015)
5. L. Panbo, H. Ying, Z. Xiang, Superparamagnetic NiFe₂O₄ particles on poly(3,4-ethylenedioxythiophene)-graphene: Synthesis, characterization and their excellent microwave absorption properties. *Compos. Sci. Technol.* **95**, 107–113 (2014)
6. M. Khairy, Synthesis, characterization, magnetic and electrical properties of polyaniline/NiFe₂O₄ nanocomposite. *Synth. Met.* **189**, 34–41 (2014)
7. J. Yan, Y. Huang, X. Chen, C. Wei, Conducting polymers-NiFe₂O₄ coated on reduced graphene oxide sheets as electromagnetic (EM) wave absorption materials. *Synth. Met.* **221**, 291–298 (2016)
8. M. Ajmal, M.U. Islam, Structural, optical and dielectric properties of polyaniline-Ni_{0.5}Zn_{0.5}Fe₂O₄ nano-composites. *Phys. B* **521**, 355–360 (2017)
9. A.M.A. Henaish, A.S. Abouhaswa, Effect of WO₃ nanoparticles doping on the physical properties of PVC polymer. *Bull. Mater. Sci.* **43**, 149 (2020)
10. J.C. Apesteguy, P.G. Bercoff, S.E. Jacobo, Preparation of magnetic and conductive Ni-Gd ferrite-polyaniline composite. *Phys. B* **398**, 200–203 (2007)
11. A.C.V. de Araujo et al., Synthesis, characterization and magnetic properties of polyaniline-magnetite nanocomposites. *Synth. Met.* **160**, 685–690 (2010)
12. B. Senthilkumar, K. Vijaya Sankar, C. Sanjeeviraja, R. Kalai Selvan, Synthesis and physico-chemical property evaluation of PANI-NiFe₂O₄ nanocomposite as electrodes for supercapacitors. *J of Alloys and Compounds* **553**: 350–357 (2013).
13. C. Wang, Y. Shen, X. Wang, H. Zhang, A. Xie, Synthesis of novel NiZn-ferrite/Polyaniline nanocomposites and their microwave absorption properties. *Mater. Sci. Semicond. Process.* **16**, 77–82 (2013)
14. A.H. Elsayed, M.S. Mohy Eldin, A.M. Elsyed, A.H. Abo Elazm, E.M. Younes, Motaweh, Synthesis and Properties of Polyaniline/ferrites Nanocomposites. *Int. J. Electrochem. Sci.* **6**, 206–221 (2011)
15. J. Zhoua, Synthesis and electromagnetic property of Li_{0.35}Zn_{0.3}Fe_{2.35}O₄ grafted with polyaniline fibers. *Appl. Surf. Sci.* **420**, 154–160 (2017)
16. M. Bakr, Karimat EL-Sayed, Structural, magnetic and dielectric properties of (PANI)-Ni_{0.5}Zn_{0.5}Fe_{1.5}Cr_{0.5}O₄ nanocomposite. *Compos. B* **56**, 270–278 (2014)
17. S. Sultana, Rafiuddin, Mohammad Zain Khan, Khalid Umar, Synthesis and characterization of copper ferrite nanoparticles doped polyaniline. *J. Alloy. Compd.* **535**, 44–49 (2012)
18. A.M.A. Henaish, M. Mostafa, B.I. Salem, O.M. Hameda, Improvement of magnetic and dielectric properties of magneto electric BST-NCZMF nano-composite. *Phase Transitions* **93**, 470–490 (2020)
19. S.A. Ebrahima, M.E. Harbb, M.M. Solimana, M.B. Tayelb, Preparation and characterization of a pseudocapacitor electrode by spraying a conducting polymer onto a flexible substrate. *J. of Taibah University for Science* **10**, 281–285 (2016)
20. A. Baykal, M. Gunay, M.S. Toprak, H. Sozeri, Effect of ionic liquids on the electrical and magnetic performance of polyaniline-nickel ferrite nanocomposite. *Mater. Res. Bull.* **48**, 378–382 (2013)
21. C. Liu, H. Tai, P. Zhang, Z. Yuan, X. Du, G. Xie, Y. Jiang, A high-performance flexible gas sensor based on self-assembled PANI-CeO₂ nanocomposite thin film for trace-level NH₃ detection at room temperature. *Sensors and Actuators B* **261**, 587–597 (2018)
22. A.M.A. Henaish, Physical and spectral studies of Mg-Zn ferrite prepared by different methods. *Arab. J. Nucl. Sci. Appl.* **53**(1), 9–18 (2019)
23. O.M. Hameda, A. Tawfik, M.A. Amer, B.M. Kamal, D.E. El Refaay, DC conductivity and magnetic properties of piezoelectric-piezomagnetic composite system. *J. Magn. Magn. Mater.* **324**, 3229–3237 (2012)
24. C. Tanasoiu, I. Nicolae, P. Nicolau, H. Niculescu, C. Mihaiache, A new type of thermostat of high stability using a magnetic temperature transducer. *J. Phys. E: Sci. Instr.* **18**, 50 (1985)
25. C. Venkataraju, G. Sathishkumar, K. Sivakumar, Effect of Cd on the structural, magnetic and electrical properties of nanostructured Mn-Zn ferrite. *J. Magn. Magn. Mater.* **323**, 1817–1822 (2011)
26. Y. Zhi, A. Chen, Maxwell-Wagner polarization in ceramic composites BaTiO₃-(Ni_{0.3}Zn_{0.7})Fe_{2.1}O₄. *J. of Applied Physics* **9**(1), 794 (2002)
27. A.A. Sattar, H.M. El-Sayed, K.M. El-Shokofy, M.M. El-Tabey, Improvement of the Magnetic Properties of Mn-Ni-Zn Ferrite by the Non-magnetic Al³⁺-Ion Substitution. *J. App. Sci.* **5**(1), 162–168 (2005)

28. U.S. Sharma, R. Shah, Study of polyaniline coated CuFe₂O₄ nanoparticles and their application in biosensor. *AIP Conf. Proc.* **1728**, 020275 (2016)
29. A. Tawfik, O.M. Hemeda, A.M.A. Henaish, A.M. Dorgham, High Piezoelectric Properties of Modified Nano Lead Titanate Zirconate Ceramics. *Mater. Chem. Phys.* **211**, 1–8 (2018)
30. D.K. Bandgar, S.T. Navale, S.R. Nalage, R.S. Mane, F.J. Stadler, D.K. Aswal, S.K. Gupta, V.B. Patil, Simple and low-temperature polyaniline-based flexible ammonia sensor: a step towards laboratory synthesis to economical device design. *J. Mater. Chem.* **3**, 9461–9468 (2015)
31. O.M. Hemeda, A.M.A. Henaish, B.I. Salem, F.S. El-Sbakhly, M.A. Hamad, The dielectric and magnetic properties of RTV-silicon rubber Ni–Cr ferrite composites. *Appl. Phys. A.* **126**, 121 (2020)
32. N. Raghuram, T.S. Rao, K.C.B. Naidu, Investigations on functional properties of hydrothermally synthesized Ba_{1-x}Sr_xFe₁₂O₁₉ (x= 0.0–0.8) nanoparticles. *Appl. Phys. A* **125**(839), 1–15 (2019)
33. A.M. Shaikh, S.C. Watawe, S.S. Bellad, S.A. Jadhav, B.K. Chougule, Microstructural and magnetic properties of Zn substituted Li–Mg ferrites. *Mater. Chem. Phys.* **65**, 46–50 (2000)
34. T.H. Ting, R.P. Yu, Y.N. Jau, Synthesis and microwave absorption characteristics of polyaniline/NiZn ferrite composites in 2–40 GHz. *Mater. Chem. Phys.* **126**, 364–368 (2011)
35. S. Mazen, M. Abdallah, R. Nakhla, H. Zaki, F. Metawe, *Mater. Chem. Phys.* **34**, 35–40 (1993)

Publisher's Note Springer Nature remains neutral with regard to jurisdictional claims in published maps and institutional affiliations.